Title
PREPARATION, CHARACTERIZATION, AND PHOTOELECTRDNIC PROPERTIES OF GERMANIUM SUBSTITUTED SINGLE CRYSTALS

Author
Sieber, K.D.

Publication Date
1984-08-01

Lawrence Berkeley Laboratory
UNIVERSITY OF CALIFORNIA

Materials & Molecular Research Division

Submitted to the Journal of the Chemical Society,
Faraday Transactions

PREPARATION, CHARACTERIZATION, AND PHOTOELECTRONIC PROPERTIES OF GERMANIUM SUBSTITUTED Fe_2O_3 SINGLE CRYSTALS

K.D. Sieber, C. Sanchez, J.E. Turner,
and G.A. Somorjai

August 1984

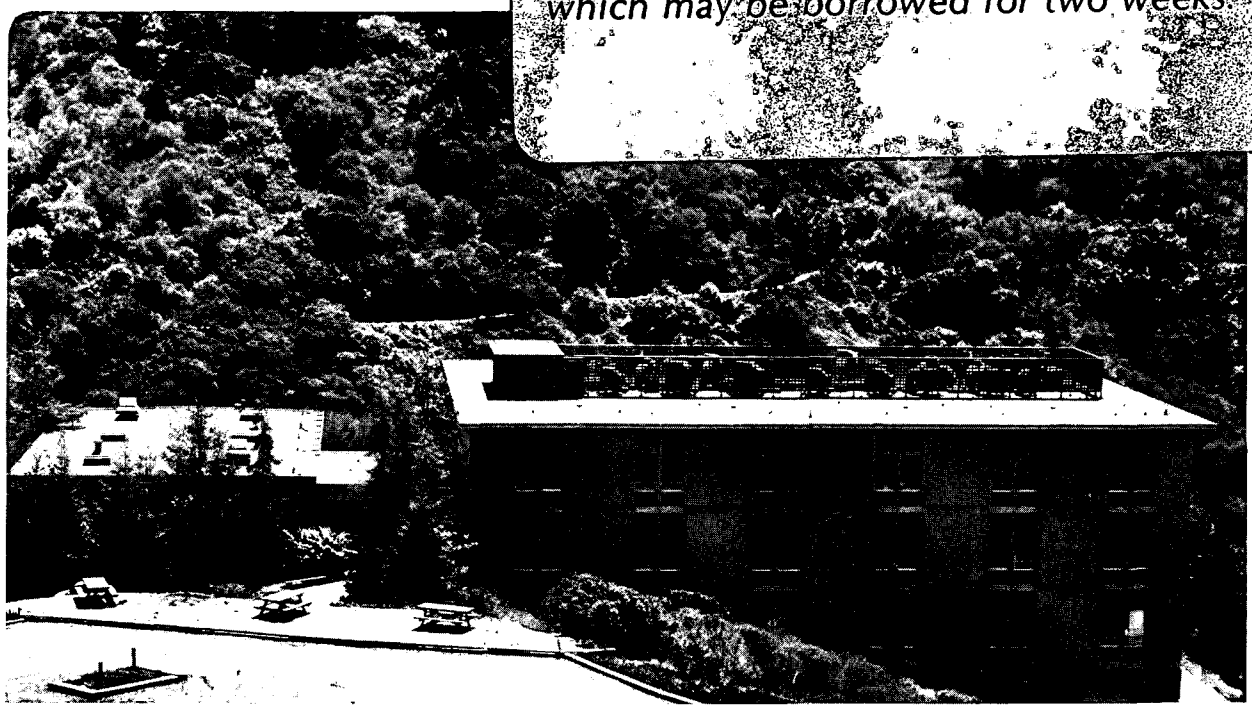

Prepared for the U.S. Department of Energy under Contract DE-AC03-76SF00098

DISCLAIMER

LBL-18033

PREPARATION, CHARACTERIZATION, AND PHOTOELECTRONIC PROPERTIES OF GERMANIUM SUBSTITUTED Fe_2O_3 SINGLE CRYSTALS

K.D. Sieber, C. Sanchez, J.E. Turner and G.A. Somorjai

Materials and Molecular Research Division,
Lawrence Berkeley Laboratory, and
Department of Chemistry, University of California,
Berkeley, California, 94720 USA

PREPARATION, CHARACTERIZATION, AND PHOTOELECTRONIC PROPERTIES OF GERMANIUM SUBSTITUTED Fe_2O_3 SINGLE CRYSTALS

K.D. Sieber, C. Sanchez, J.E. Turner and G.A. Somorjai

Materials and Molecular Research Division,
Lawrence Berkeley Laboratory, and
Department of Chemistry, University of California,
Berkeley, California, 94720 USA

ABSTRACT

Single crystals of germanium substituted Fe_2O_3 were grown using chemical vapor transport with tellurium tetrachloride and their crystallographic, electrical magnetic, and photoelectronic properties were measured. Germanium substituted Fe_2O_3 crystallized with the corrundum structure and is an extrinsic n-type semiconductor with a room temperature resistivity of around 5 Ω cm and an impurity ionization energy of 0.12 eV. Low temperature susceptibility measurements suggest that insertion of Ge(IV) leads to reduction of iron(III) to iron(II) without spinel phase inclusion. Photoelectrochemical measurements and determinations of the flatband potential by different techniques suggest that the behavior of Fe_2O_3 photoanodes may be influenced by energy levels in the bandgap near the conduction band.

Introduction

Iron oxides have recently been investigated as possible electrode materials for the photoelectrolysis of water using sunlight.[1] In an overview, the large adsorption coefficients[2] and favorable bandgap (~2.2 eV) of α-Fe_2O_3[3] suggest that a large portion of the solar spectrum could be used efficiently in an iron oxide based semiconductor-liquid junction p-n assembly. Most of the studies using n-type Fe_2O_3 photoanodes have focused on thin films[4] or polycrystalline sintered disks[5] primarily because of the ease of sample preparation, and it was found that iron oxides might be useful if the quantum efficiency of this material could be improved. The origin of the low quantum efficiency of Fe_2O_3 is unclear because the inhomogeneities of thin films or polycrystalline materials make it difficult to separate bulk effects from surface properties.

One of the main problems associated with the application of Fe_2O_3 photoanodes is the intrinsic high resistivity of the hematite corundum phase. Photoelectrolysis processes require high conductivity semiconducting materials, and, unlike the binary oxides TiO_2 or WO_3, the corundum phase of iron oxide has a low tolerance for deviations from an M_2O_3 stoichiometry.[6] As a result, it is understandably difficult to prepare homogeneous semiconducting samples. It has been proposed that the conductivity of undoped Fe_2O_3 is actually due to Fe_3O_4 phase inclusions.[6] These phase inclusions are characteristic of an inhomogeneous material and it has been shown that spinel inclusions can also decrease the quantum efficiency of Fe_2O_3 photoanodes by promoting extensive recombination of photogenerated electron-hole pairs.[6] It is possible to prepare ternary solid solutions of Fe_2O_3 with other binary oxides, such as TiO_2,[7] which are conducting without spinel phase inclusions.

The homogeneity of these ternary compounds offers the advantage of being able to examine the importance of bulk effects such as grain boundaries, or surface properties such as surface states, in photoelectrolysis processes without interference from extraneous phase inclusions in Fe_2O_3.

Among the more interesting ternary oxides involving Fe_2O_3 are the solid solutions between Fe_2O_3 and SiO_2 or GeO_2. Although silicon doped iron oxides have been used as photoanodes,[8] they are difficult to prepare as homogeneous materials due to the refractory nature of silicon dioxide; however, Sanchez and coworkers were able to prepare the solid solution $Fe_{2-x}Ge_xO_3$ as polycrystalline sintered disks using gel techniques.[9] Sanchez suggested that the limit of solubility of GeO_2 in Fe_2O_3 is less than or equal to five mole percent, and showed that the conducting solid solution has photoelectrochemical properties which are similar to those of Fe_2O_3 found in the literature. More recently Agafonov et al demonstrated that single crystals of $Fe_{2-x}Ge_xO_3$ could be grown by chemical vapor transport techniques.[10] The results of Sanchez and those of Agafonov suggest that high quality conducting single crystals of $Fe_{2-x}Ge_xO_3$ can be prepared and that this material would be sufficiently homogeneous so that the photoelectronic properties of conducting Fe_2O_3 could be examined without interference from grain boundaries or phase inclusions.

In this paper we report the preparation of single crystals of $Fe_{2-x}Ge_xO_3$ ($x \leq 0.02$) by chemical vapor transport as well as the characterization of the crystallographic, electrical, magnetic, and photoelectronic properties of these samples. It was found that single crystals of germanium substituted Fe_2O_3 crystallize with the corundum structure and are extrinsic n-type semiconductors. In addition, the photoelectronic properties of

$Fe_{2-x}Ge_xO_3$ crystals suggest the presence of a sub-band gap energy level which may influence the photoelectrochemical behavior of Fe_2O_3 to a large extent.

Experimental

Single crystals of germanium substituted Fe_2O_3 were prepared by chemical vapor transport using tellurium(IV) tetrachloride as a transport agent. Approximately 1 gram of charge consisting of Fe_2O_3 (MCB reagent) with 1 mole percent of elemental germanium was placed in a 15cm x 13mm I.D. silica tube along with approximately 20mg of Te metal. The tube was then evacuated to below 1 micron and backfilled with 400 Torr of chlorine gas then sealed. An identical procedure was used to prepare pure Fe_2O_3 crystals for comparison, except that the addition of germanium to the charge was omitted. The tubes were then placed in three zone transport furnace and after 24 hours of back transport from 800°C to ~450°C the charge was transported for one week. The temperature of the charge zone was 885°C and that of the growth zone 790°C. After one week the furnace was turned off and left to cool to room temperature. The tubes were then removed from the furnace, opened under vacuum, and the product washed with dilute nitric acid, rinsed with water, then dried with acetone. Platelets as large as 5 x 2 x 0.01mm were grown using this technique, and the major face of the crystals, as determined by X-ray diffraction was the (001) basal plane.

X-ray powder diffraction was performed on ground single crystal powders using a Siemens model D500 powder diffractometer equipped with monochromated Cu $k\alpha_1$ radiation. Fast scans were carried out using a scan rate of 6° 2θ/min for phase identification. Slow scans for

lattice parameter determination were carried out using a scan rate of 0.5° 2θ/min and lattice parameters were calculated using a least squares refinement technique with the aid of a computer. All cell parameters were calculated using hexagonal indexing, and all crystalline directions referred to hereafter are with reference to the hexagonal unit cell.

The electrical properties of samples were measured using the Van der Pauw[11] four probe technique and all crystals were measured in the (001) basal plane. Contacts to the samples were made using an indium-gallium eutectic and the ohmicity of the contact was verified by repetitive measurement of the resistivity at several different current magnitudes between 10μA and 100mA. The variation of the electrical resistivity with temperature was measured using the same techniques except that the ohmic contacts were provided by ultrasonic soldering of pure indium metal. The carrier type of the conducting crystals was determined by qualitative measurement of the Seeback voltage at room temperature.

The magnetic properties of ground single crystal powders were investigated using an S.H.E. Corporation "SQUID" susceptometer. The magnetic susceptibility of samples was measured at varying field strengths between 5 and 25kG in the temperature region between 200K and 10K to examine the field dependence of the sample susceptibility at various temperatures.

Electrodes of germanium substituted Fe_2O_3 were prepared by mounting the crystals on a copper plate with an indium-gallium eutectic to provide an ohmic contact. The copper plate was attached to a glass sheathed metallic lead, and the entire assembly was insulated with a silicon resin

so that only the (001) basal plane of the crystal was exposed. During the electrochemical experiments the electrode was suspended in solution and periodically examined for changes in dark currents which could be indicative of leaks in the insulation.

The photoelectrochemical properties of samples were investigated using an Pine RDE-3 potentiostat in a standard three electrode configuration with a platinum counter electrode and an S.C.E. reference electrode in an all quartz cell. Two types of illumination sources were used: a 300W tungsten-halogen lamp or a 150W high pressure Xenon arc lamp. D.C. photocurrent experiments were performed with illumination from the tungsten-halogen lamp, which was passed through an I.R. filter then focused on the sample. The intensity of the focused light in this technique was approximately 30mW/cm^2 as determined with a calibrated Epply thermopile. A.C. experiments were carried out using Xenon arc lamp illumination which was passed through an I.R. filter and a monochromator before being focused with a quartz lens on the sample. For A.C. measurements using monochromatic radiation a Bulova tuning fork chopper (model 140C) operating at 150 Hz was mounted at the exit slit of the monochromator. The A.C. photocurrent was detected using a PAR model 124 lock-in amplifier equipped with a model 117 preamp operating in the differential mode. For rectified photocurrent measurements a 0 - 10 V voltage rectifier was employed in the manner indicated in reference 16. Quantum efficiencies were determined by calculating the number of electrons generated in the A.C. photocurrent per number of photons striking the semiconductor surface. The photon flux was measured with the same A.C. techniques using a calibrated silicon photodiode.

Capacitance measurements were carried out using the method of Horowitz[12] with the equipment previously described by measuring that part of a 10 - 20 mV A.C. signal passing through the cell which was in quadrature with the initial reference phase.

Electrochemical investigations were done in two media: 1 molar NaOH and 1 millimolar quinhydrone in 1 molar NH_4NO_3. The basic solutions were prepared using distilled deionized water and Mallinckrodt Analytical grade NaOH pellets. The experiments with quinhydrone required a neutral media to avoid decomposition of the couple, and 1 molar NH_4NO_3 served as an electrolyte to provide sufficient solution conductivity. For experiments utilizing the quinhydrone redox couple, recrystallized quinhydrone was used and all work was done under argon to avoid oxidation of the couple during the experiments. All voltages herein will be reported relative to the saturated calomel electrode (S.C.E.) whose potential is 0.242 V relative to the normal hydrogen electrode.

Results and Discussion

I) Preparation and Crystallography

The results of the crystal growth experiments show that germanium substituted Fe_2O_3 can be grown under the same conditions as pure Fe_2O_3. Alpha-Fe_2O_3 itself crystallizes with the corundum structure which can be described as a hexagonal close packed array of oxygen anions in which two thirds of the octahedral interstices are occupied by cations. X-ray diffraction powder patterns of the substituted and pure ground single crystals indicated single phase corundum patterns in all cases. It was concluded that the germanium substituted and pure materials are therefore isostructural. The major face of the single crystal platelets was the

(001) basal plane, and the least squares lattice parameters determined for the substituted and unsubstituted materials are listed in Table 1 along with some supplementary results for comparison.

It is seen in Table 1 that the lattice parameters of germanium substituted Fe_2O_3 are virtually in the same as those of pure Fe_2O_3. The results are in good agreement with the examples given for single crystals prepared by similar techniques. The crystallographic results are insufficient to determine either the composition of the solid solution or the site occupancy of germanium in the corundum lattice; however, elemental analysis of the crystals using a scanning electron microscope equipped with a Kevex probe showed germanium at the limit of detection of the instrument in the substituted crystals. The detection limit of the Kevex probe used was about one atomic percent, and these results suggest that the germanium concentration in the substituted crystals is around two mole percent or less. Agafonov suggested on the basis of neutron activation analysis that the solubility limit of GeO_2 in Fe_2O_3 is near two mole percent.[10] Thus, it is likely that the apparent lack of change in the lattice parameters of the germanium substituted Fe_2O_3 relative to the pure phase is due to the small amount of germanium substitution.

II) Electrical Properties

Room temperature resistivity measurements of germanium substituted and pure Fe_2O_3 show a dramatic difference between the two materials: the incorporation of germanium into the Fe_2O_3 lattice lowers the resistivity of Fe_2O_3 by at least six orders of magnitude. The resistivity of single crystals of $Fe_{2-x}Ge_xO_3$ ($x \leq 0.02$) is 5 ± 4 Ω cm while that of pure Fe_2O_3 crystals grown under the same conditions is greater than 10^6 Ω cm.

Qualitative measurements of the Seebeck voltage showed the substituted material to be an n-type semiconductor.

The plot of log ρ versus 1/T between 77 and 300K for germanium substituted Fe_2O_3 is shown in Figure 1. The impurity ionization energy which can be calculated from the slope of this graph is 0.12 eV. This value is much less than the optical bandgap of Fe_2O_3, therefore, the electrical properties of germanium substituted Fe_2O_3 indicate that it is an extrinsic n-type semiconductor. These results are consistent with the interpretation that the insertion of Ge(IV) in the corundum structure leads to a reduction of iron(III) to iron(II). Conduction can be considered to occur via electron hopping between iron(II) and iron(III), and the observed activation energy is consistent with that reported for other mixed valence iron oxides.[13] These results are also consistent with those of Sanchez et al who found that the resistivity of the solid solution between Fe_2O_3 and GeO_2 decreases with increasing GeO_2 content.[9]

III) Magnetic Properties

Although the X-ray diffraction patterns of the single crystal powders indicated that the corundum structure was the only phase present, the possibility exists that Fe_3O_4 phase inclusions beyond the detection limit of diffraction might be present because Fe_3O_4 phase inclusions in Fe_2O_3 will also produce a semiconducting material. The presence of Fe_3O_4 phase inclusions in Fe_2O_3 can be detected by measuring the magnetic susceptibility of a material at various field strengths. If Fe_3O_4 is present, a Honda-Owens Plot of susceptibility versus the reciprocal field strength will show a positive slope which will persist with decreasing temperature. Thus, to investigate the possibility of spinel phase inclusions in the

single crystals the magnetic properties of single crystal powders were examined.

The Honda-Owens plots representing the variation of magnetic susceptibility with reciprocal field strength at different temperatures below 200K for substituted and pure Fe_2O_3 are presented in Figure 2. Although the magnitude of the susceptibility of the two samples is the same, germanium substituted Fe_2O_3 shows a weak field dependence which decreases with decreasing temperature. If Fe_3O_4 phase inclusions were present in this material a constant field dependence at different temperatures should be expected with little or no interference from Fe_2O_3 because hematite is antiferromagnetically ordered in this temperature region, as verified in Figure 2, and the experiments were performed well below the Curie temperature of Fe_3O_4.

The magnetic properties of germanium substituted Fe_2O_3 are not consistent with spinel phase inclusions and can be interpreted as indicating weak ferrimagnetism or parasitic paramagnetism.[14] These results suggest that the substituted material is homogeneous with magnetic properties most likely arising from itinerant electrons associated with iron(II) in the corundum lattice. In principle, if this material obeyed the Curie-Weiss relation in this temperature region the extent of charge compensation resulting from germanium substitution could be estimated from μ_{eff}; however, this analysis is not justified in light of the apparent complexity of the magnetic behavior.

IV) Photoelectronic Properties

Photoelectrochemical investigations were performed on the (001) basal plane of the germanium substituted α-Fe_2O_3 crystals in one molar NaOH solutions. Cyclic voltammograms registered in the dark showed dark currents well below five microamperes per cm^2 in the region between -1.0 and 0.7 V versus the S.C.E.. At potentials more cathodic or anodic of these values larger dark currents were observed. The cathodic dark current is presumably related to hydrogen evolution, while the anodic current is probably related to a breakdown of the diode behavior resulting in the oxidation of water to oxygen gas. This behavior is characteristic of an n-type photoelectrochemical diode.

D.C. voltammograms under illumination using a tungsten-halogen lamp with slow chopping of the light beam showed photocurrents on the order of 500 $\mu A/cm^2$ at 0.5 V versus the S.C.E. as shown in Figure 3. These photocurrents are most likely due to the photosensitized electrolysis of water or hydroxide ion to O_2 at the semiconductor surface. Continuous cycling experiments showed that material appeared stable under illumination and no tarnishing of the crystal surface was observed. The qualitative behavior of the single crystal electrodes is in good agreement with that of polycrystalline materials reported in the literature except that no photocathodic currents were ever observed at potentials negative of the photocurrent onset potential.

A plot of the quantum efficiency versus wavelength at zero bias for germanium substituted Fe_2O_3 is shown in Figure 4. The quantum efficiencies of all crystals measured was on the order 0.005 to 0.1 in the region between 600 and 350nm. The bandgap information which can be extracted

from these results show the lowest interband optical transition, which has previously been characterized as indirect,[15] to be located at about 550nm. This corresponds to a value of about 2.2 eV, in good agreement with literature values. The low quantum efficiencies reported here have been observed by numerous investigators and appear typical of hematite photoanodes.

The photocurrent onset potential of germanium substituted Fe_2O_3 was determined using A.C. techniques, and the results were analyzed using the method of Ginley and Butler.[17] The graph of I_{ph}^2 versus voltage, shown in Figure 5, has an x axis intercept at approximately -0.500 V versus the S.C.E. at pH 14. It may be concluded on the basis of these results that the flatband potential of germanium doped Fe_2O_3 indicated by photocurrent measurements is in good agreement with the literature values of -0.6 V determined by capacitance measurements of both polycrystalline materials and single crystal samples such as the (111) face of Zr doped Fe_2O_3[12] and the (012) face of Pb doped Fe_2O_3.[18]

As an additional check of the flatband potential, capacitance measurements were performed at 10kHz using the method of Horowitz.[12] The Mott-Schottky plot for these experiments is shown in Figure 6. There are two features in this plot: first, an x axis intercept of approximately -0.95 V and secondly, an apparent change in slope at about -0.6V. The intercept of the Mott-Schottky plot indicates a flatband potential of around -0.95 V and is in good agreement with the calculations of Horowitz[12] and the measurements of Gissler.[4c] The apparent change of slope in the plot is similar to that observed by Kennedy and coworkers[7] and has been ascribed to deep lying impurity levels in the bandgap. It is believed that these levels become occupied at biases cathodic of where the change

in slope occurs, thus changing the capacitance of the space charge layer. There is a close coincidence between the photocurrent onset potential and the potential where the slope of the Mott-Schottky curve changes. This suggests that the deep lying impurity levels must be ionized before photoelectrolysis can occur.

Given the flatband potential, the activation energy from the electrical measurements, and the relative position of the donor levels as indicated on the Mott-Schottky plot, a hypothetical energy diagram may be constructed for germanium substituted Fe_2O_3 in the (001) zone. This diagram is presented in Figure 7, and is similar to that presented by Kennedy and coworkers.[7]

To investigate the role of the impurity levels during photoelectrochemical processes at the Fe_2O_3 surface a redox couple was chosen whose potential is close to that of the postulated donor levels. The potential of the quinhydrone redox couple, 0.699 V versus the N.H.E., fits this criterium. This couple has a potential which is pH independent with respect to the hydrogen couple except in alkaline solution where decomposition of the couple occurs. The quinhydrone couple lies slightly below the postulated donor levels in Fe_2O_3, and if these were electrochemically active this might be observed with quinhydrone.

The results of the quinhydrone experiments are shown in Figure 8. In the dark, the quinhydrone couple shows partial rectification, as observed by Fredlein and Bard.[19] In other words, the reduction of benzoquinone is present while the oxidation of p-hydroxyphenol is not observed. The cathodic current in the dark may be interpreted as a donation of electrons from the impurity level to the solution. This will

occur if the energy distribution of the oxidized species overlaps the position of the impurity energy level at the semiconductor surface. When the electrochemical potential of the semiconductor lies cathodic of the impurity level, the impurity level will be occupied and may donate electrons to oxidized species at the surface. Oxidation of reduced species not be observed if the energy of the reduced species lies sufficiently anodic of the sub-bandgap energy level. Thus, the behavior of the quinhydrone couple in the dark is consistent with the previously proposed energy diagram for germanium substituted Fe_2O_3.

The behavior of the quinhydrone couple under illumination is more complex due to the presence of two oxidizable species in solution: p-hydroxyphenol and water. Under illumination with white light only an anodic photocurrent is observed. The anodic photocurrent is most likely due to a combination of the photosensitized oxidation of both reduced species in solution. In fact, the increase in the cathodic current indicative of the reduction of benzoquinone shown clearly that p-hydroxyphenol is being oxidized near the semiconductor surface; however, it possible that this oxidation may be mediated by an intermediate species such as hydroxyl radical because the H_2O/O_2 couple lies closer to the valence band of Fe_2O_3 than p-hydroxyphenol and therefore the oxidation of water is more energetically feasible. This hypothesis is also supported by the fact that the oxidation of p-hydroxyphenol is known to be slow and not controlled by diffusion,[19] as shown in Figure 8.

The electrical properties of germanium doped Fe_2O_3, coupled with the results of the quinhydrone experiments and the measurements of the apparent flatband potential using both capacitance and photocurrent techniques,

suggest that the efficiency of Fe_2O_3 photoanodes is limited by the bulk electronic structure of the material. The presence of a sub-bandgap energy level below the conduction band of Fe_2O_3 is an intrinsic characteristic of the electronic structure, and, despite the fact that this energy level apparently interferes with the efficiency of the photoelectrolysis process, it is this same energy level which is probably responsible for the semiconducting characteristics of doped Fe_2O_3 which are necessary for photoelectrolysis to occur at all. In addition, the differences between the flatband potentials measured by two different methods show that this impurity level must be depleted of carriers in the space charge region before photoelectrolysis can occur. Thus, it is suggested here that the substantial bias necessary for large photocurrents with Fe_2O_3 photoanodes is necessary to create a sufficiently large potential gradient in the space charge layer so that trapping of photogenerated electrons in this sub-bandgap energy level may be overcome.

Other authors have discussed the problems of backreactions occuring at Fe_2O_3 photoanodes[19,20] and it is possible that the backreactions, as evidenced by transient cathodic spikes in the chopped photocurrent curves, are mediated through the proposed sub-bandgap energy level. Furthermore, it has been proposed that the transfer of holes to the surface of Fe_2O_3 may proceed via deep lying iron e_g^2 energy levels in the bandgap near the valence band.[21] This would imply that recombination processes in the space charge region of Fe_2O_3 could be extensive because of the possibility of very low hole mobility in addition to electron trapping.

Conclusion

It has been shown that the ternary solid solution $Fe_{2-x}Ge_xO_3$ where $0 < x \leq 0.02$ can be grown as single crystals by chemical vapor transport. Germanium substituted Fe_2O_3 crystallizes with the corundum structure and is an extrinsic n-type semiconductor having a room temperature resistivity of $5 \pm 4\ \Omega$ cm and an activation energy of about 0.12 eV. Magnetic susceptibility studies suggest that the conductivity of the samples arises from charge compensation resulting from reduction of iron(III) to iron(II) upon substitution of Ge(IV) in the structure. Thus, a homogeneous conducting corundum phase of Fe_2O_3 can be prepared through the use of this ternary solid solution.

The photoelectronic properties of germanium substituted Fe_2O_3 crystals suggest that the low quantum efficiency of Fe_2O_3 photoanodes is related to energy levels near the conduction band of Fe_2O_3. The low quantum efficiency cannot be explained on the basis of such effects as grain boundary recombination because the same quantum efficiency has been observed with polycrystalline samples as was found with single crystals. The comparison of the flatband potential determined by photocurrent measurements with that determined using capacitance techniques implies that an energy level near the conduction band of Fe_2O_3 must be ionized before photoelectrolysis can occur. The ionized energy level may then lead to extensive recombination of photogenerated electron-hole pairs in the space-charge layer and therefore lowered quantum efficiencies.

The deep-lying energy levels in Fe_2O_3 are most likely intrinsic characteristics of the electronic structure of this material. Electronic structure calculations[22] and optical studies of hematite[23,2] support the

idea of a complex electronic structure in the bandgap of α-Fe_2O_3; however, the influence of energy levels in the bandgap on photoelectrochemical properties of semiconductors is not well understood. α-Fe_2O_3 and many other semiconducting transition metal oxides have energy levels in the bandgap due to crystal field splitting of d-orbitals of the cation. The importance of these levels may be underestimated in interpreting the photoelectrochemical behavior of these materials.

Acknowledgements

This work was supported by the Director, Office of Energy Research, Office of Basic Energy Sciences, Chemical Sciences Division of the U.S. Department of Energy under Contract No. DE-AC03-76SF00098.

The authors gratefully acknowledge the cooperation of Dr. A. Wold of the Brown University Materials Research Laboratory for performing the measurements of electrical resistivity versus temperature, and Dr. N. Edelstein and G. Shalimoff for their assistance with the magnetic measurements on the "SQUID" susceptometer in the Materials and Molecular Research Division of the Lawrence Berkeley Laboratory.

REFERENCES

1. (a) J.H. Kennedy, R. Shinar and J.P. Ziegler, J. Electrochem. Soc. 1980, 127(10), 2307.

   (b) H.L. Sanchez, H. Steinfink and H.S. White, J. Solid State Chem. 1982, 41, 90.

   (c) C.H. Leygraf, M. Hendewerk and G.A. Somorjai, J. Catal. 1982, 78, 341.

   (d) J.E. Turner, M. Hendewerk, J. Parmeter, D. Neiman and G.A. Somorjai, J. Electrochem. Soc. 1984, in press.

2. L.A. Marasak, R. Messier and W.B. White, J. Phys. Chem. Solids 1980, 41, 981.

3. C.T. Chen and B.D. Cahan, J. Opt. Soc. Am. 1981, 71(8), 932.

4. (a) A.S.N. Murthy and K.S. Reddy, Mat. Res. Bull. 1984, 19, 241.

   (b) L.-S.R. Yeh and N. Hackerman, J. Electrochem. Soc. 1977, 124(6), 833.

   (c) J.S. Curran and W. Gissler, J. Electrochem. Soc. 1979, 126(1), 56.

   (d) S.M. Wilhelm, K.S. Yun, L.W. Ballenger and N. Hackerman, J. Electrochem. Soc. 1979, 126(3), 419.

   (e) K.L. Hardee and A.J. Bard, J. Electrochem. Soc. 1977, 124(2), 215.

   (f) R.M. Candea, Electrochim. Acta 1983, 26(12), 1803.

5. (a) R. Shinar and J.H. Kennedy, J. Electrochem. Soc. 1983, 130(2), 392.

   (b) P. Iwanski, J.S. Curran, W. Gissler and R. Memming, J. Electrochem. Soc. 1981, 128(10), 2128.

   (c) K.G. McGregor, M. Clavin and J.W. Otvos, J. Appl. Phys. 1979, 50(1), 369.

6. P. Merchant, R. Collins, K. Dwight and A. Wold, J. Solid State Chem. 1979, 27, 307.

7. (a) J.H. Kennedy and K.W. Frese, Jr., J. Electrochem. Soc. 1978, 125(5), 723.

   (b) M.P. Dare-Edwards, J.B. Goodenough, A. Hamnett and P.R. Travellick, J. Chem. Soc. Faraday Transactions 1983, 79(1) 2027.

8. J.H. Kennedy, R. Shinar and J.P. Ziegler, J. Electrochem. Soc. 1980, 127(10), 2307.

9. H.L. Sanchez, H. Steinfink and H.S. White, J. Solid State Chem. 1982, 41, 90.

10. V. Agafonov, D. Michel, M. Perez y Jorba and M. Fedoroff, Mat. Res. Bull. 1984, 19, 233.

11. L.J. Van der Pauw, Phillips Res. Rep. 1958, 13, 9.

12. G. Horowitz, J. Electroanal. Chem. 1983, 159, 421.

13. (a) R.F.G. Gardner, F. Sweet and D.W. Tanner, J. Phys. Chem. Solids 1963, 24, 1175.

(b) R.F.G. Gardner, F. Sweet and D.W. Tanner, J. Phys. Chem. Solids 1963, 24, 1183.

(c) H. Leiva, K. Dwight and A. Wold, J. Solid State Chem. 1982, 42, 41.

(d) H. Leiva, K. Sieber, B. Khazai, K. Dwight and A. Wold, J. Solid State Chem. 1982, 44, 1.

(e) J.B. Goodenough, "Metallic Oxides" in Progress in Solid State Chemistry vol 5 p 145, H. Reiss, Ed. Pergamon Press, N.Y., N.Y. (1971).

14. J.B. Goodenough, Magnetism and The Chemical Bond, pp 86-154, John Wiley and Sons, N.Y., N.Y. (1963) .

15. F.P. Koffyberg, K. Dwight and A. Wold, Solid State Comm. 1979, 30, 433.

16. J.F. McCann and J. Pezy, J. Electrochem. Soc. 1981, 128(8), 1735.

17. M.A. Butler, D.S. Ginley and M. Eibschutz, J. Appl. Phys. 1977, 48(7), 3070.

18. R.K. Quinn, R.D. Nasby and R.J. Baughman, Mat. Res. Bull. 1976, 11, 1011.

19. R.A. Fredlein and A.J. Bard, J. Electrochem. Soc. 1979, 126(11), 1892.

20. P. Iwanski, J.S. Curran, W. Gissler and R. Memming, J. Electrochem. Soc. 1981, 128(10), 2128.

21. M.P. Dare-Edwards, J.B. Goodenough, A. Hamnett and P.R. Trevellick, J. Chem. Soc. Faraday Trans. 1983, 79(1), 2027.

22. J.A. Tossel, D.J. Vaughan and K.H. Johnson, Nature 1973, 244, 42.

23. S.P. Tandon and J.P. Gupta, Spec. Lett. 1970, 3, 297.

FIGURE CAPTIONS

Figure 1 Log ρ versus 1/T for germanium substituted Fe_2O_3.

Figure 2 χ versus 1/H for Fe_2O_3 (closed circles) and germanium substituted Fe_2O_3 (open circles).

Figure 3 D.C. cyclic voltammogram for germanium substituted Fe_2O_3 electrodes in 1M NaOH with chopped illumination.

Figure 4 Quantum efficiency (η) versus wavelength for germanium substituted Fe_2O_3 at zero bias in 1M NaOH.

Figure 5 I_{ph}^2 versus voltage for germanium substituted Fe_2O_3.

Figure 6 $1/C^2$ versus voltage for germanium substituted Fe_2O_3.

Figure 7 Hypothetical energy diagram for Fe_2O_3.

Figure 8 D.C. cyclic voltammogram for germanium substituted Fe_2O_3 in 10^{-3}M quinhydrone in 1M NH_4NO_3 (dotted line - dark; solid line - under illumination).
Inset: cyclic voltammogram on platinum.

TABLE 1

Charge	a (A)	c (A)
Fe_2O_3	5.033 (2)	13.75 (1)
Fe_2O_3 + 1% Ge	5.033 (2)	13.74 (1)
Fe_2O_3 (ref. 6)	5.033	13.755
$Fe_{1.986}Ge_{0.014}O_3$ (ref. 10)	5.035 (4)	13.753 (4)

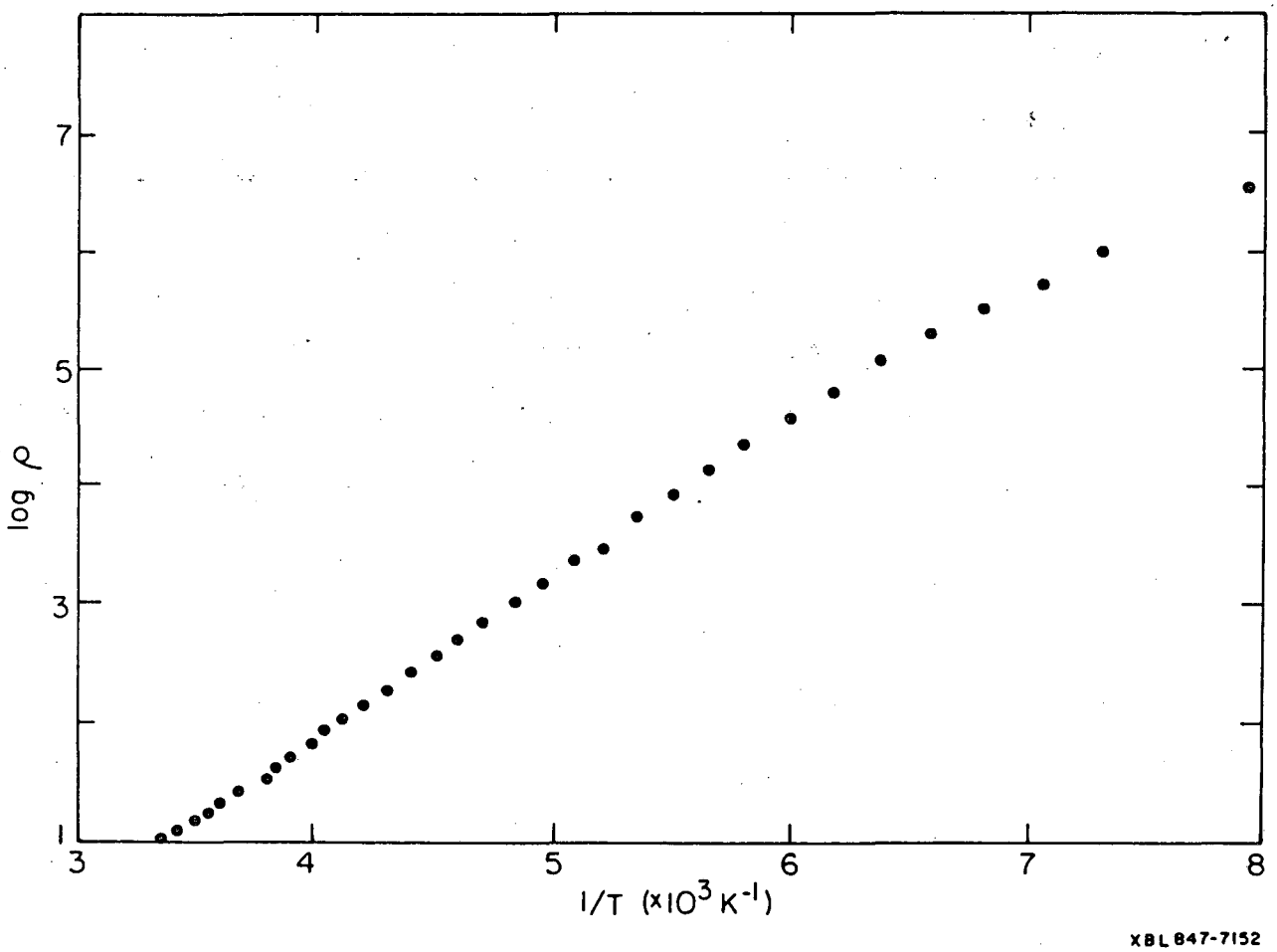

Figure 1

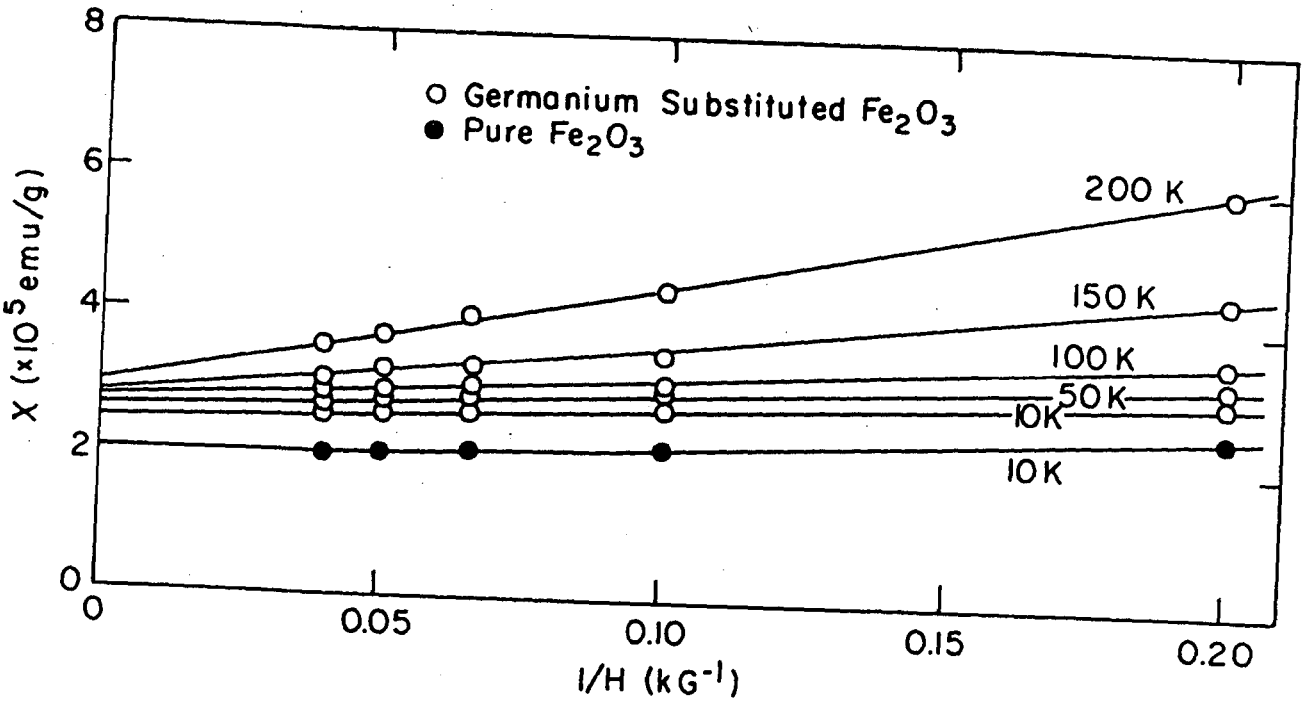

XBL 847-3250

Figure 2

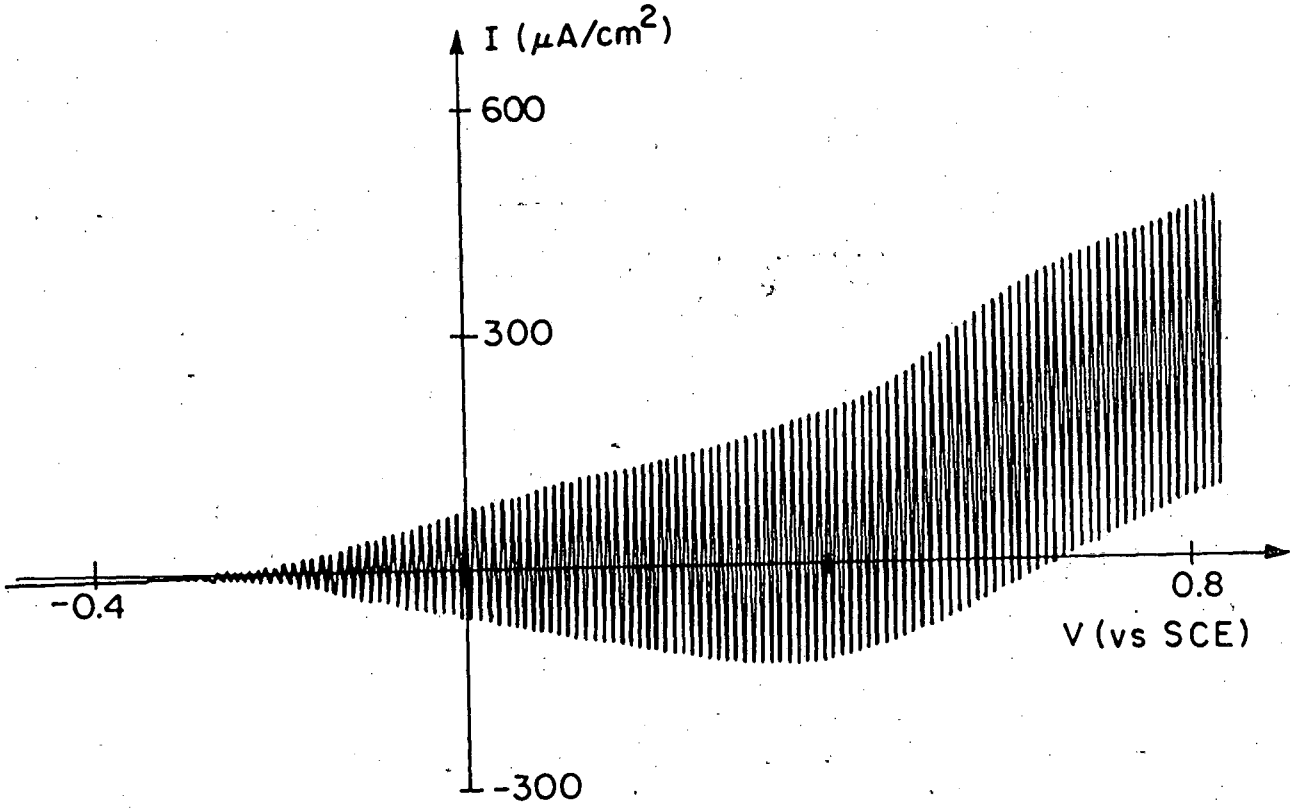

XBL 847-3247

Figure 3

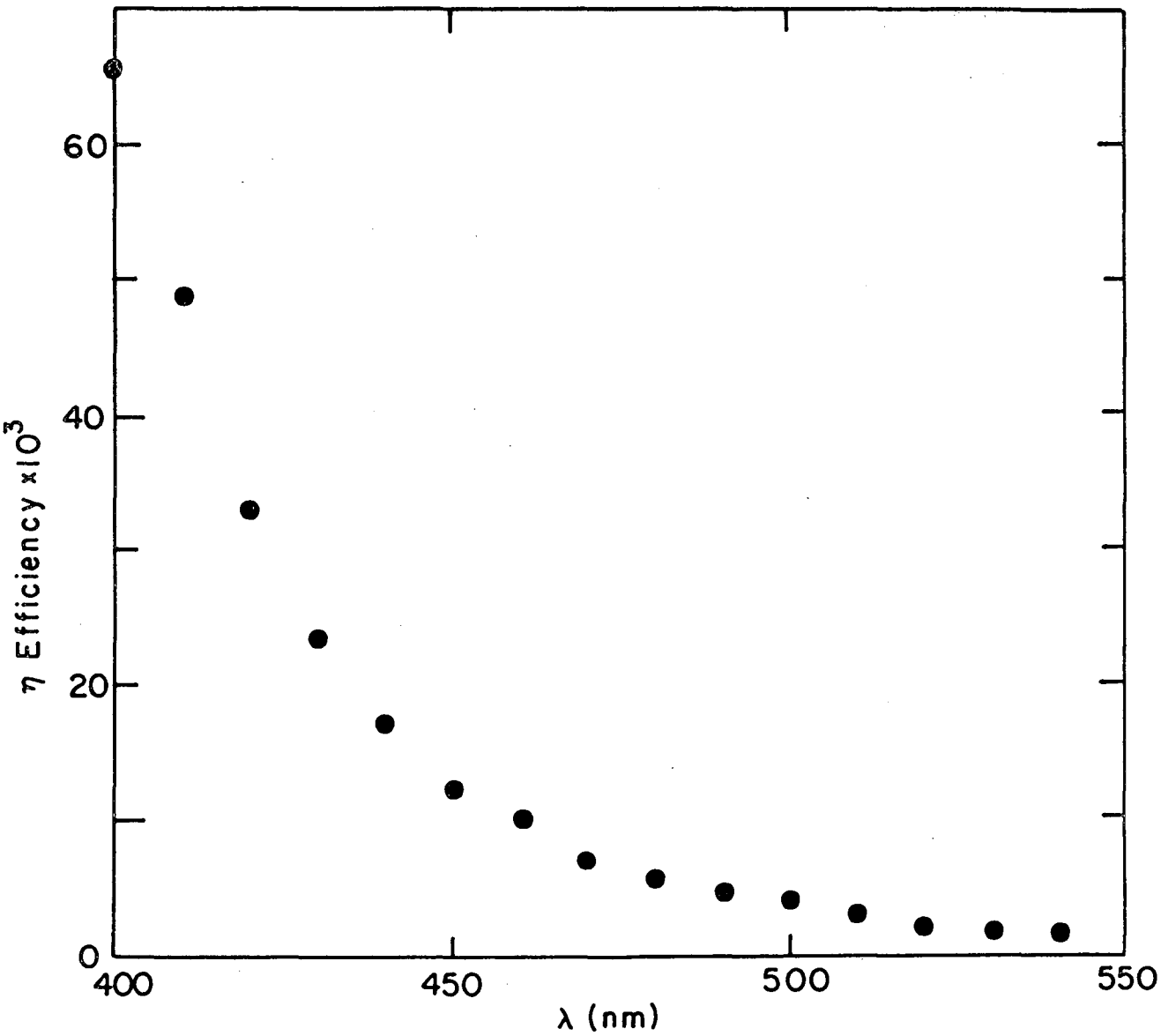

XBL 847-3249

Figure 4

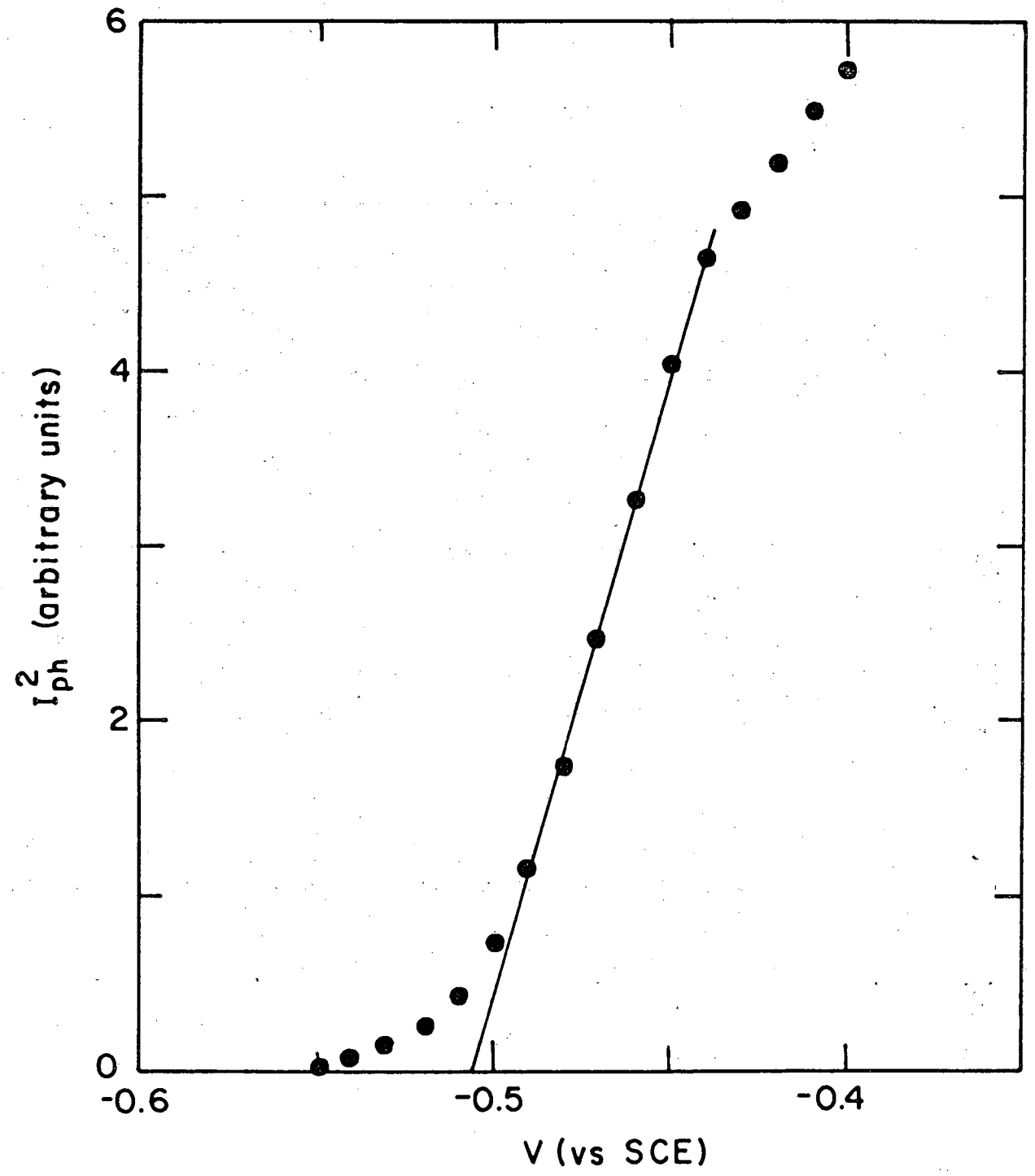

XBL 847-3248

Figure 5

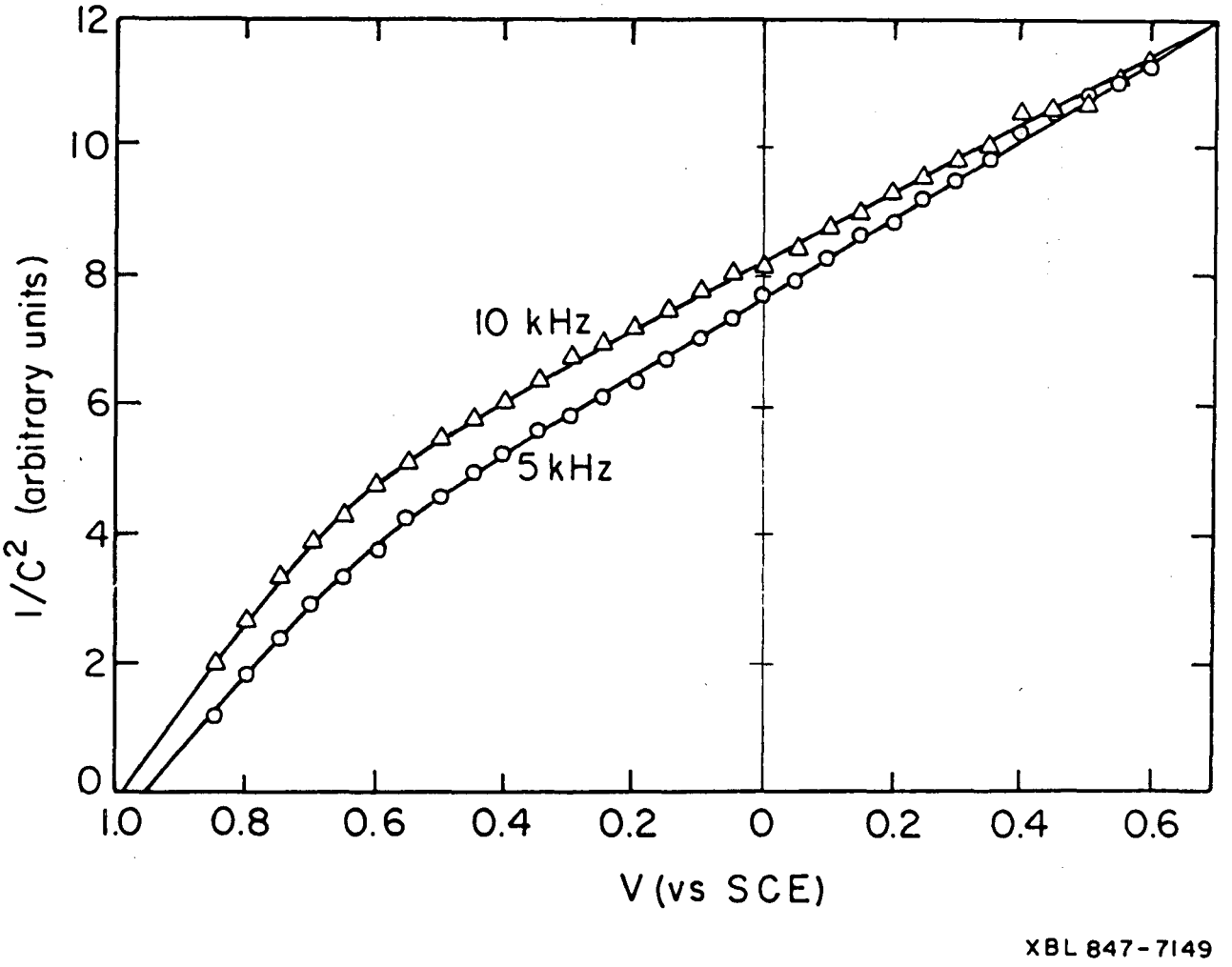
12
10
8
6
4
2
0
1.0
0.8
0.6
0.4
0.2
0
0.2
0.4
0.6
$1/C^2$ (arbitrary units)
V (vs SCE)
10 kHz
5 kHz
XBL 847-7149

Figure 6

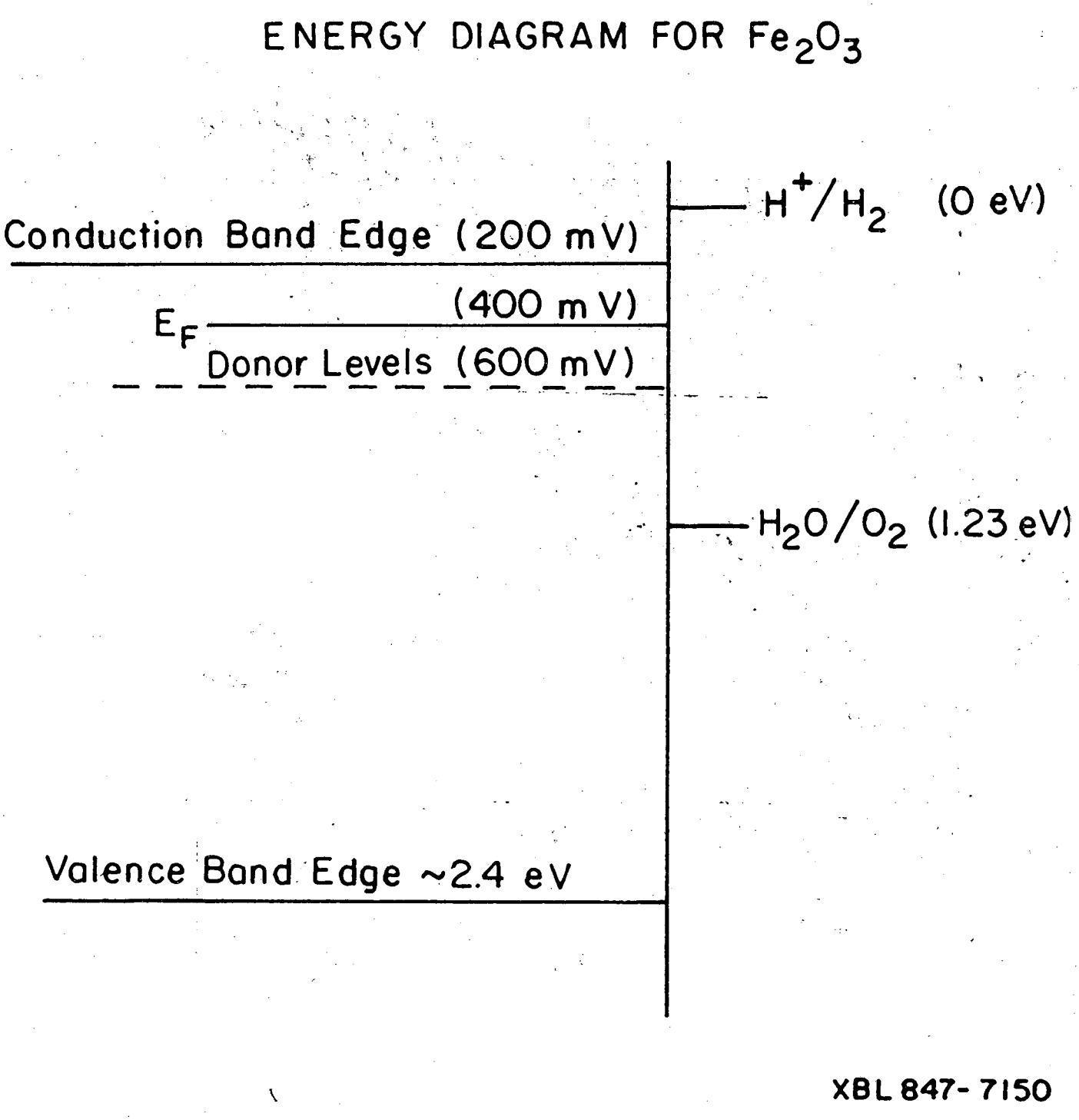
ENERGY DIAGRAM FOR Fe_2O_3
H^+/H_2 (0 eV)
Conduction Band Edge (200 mV)
(400 mV)
E_F
Donor Levels (600 mV)
H_2O/O_2 (1.23 eV)
Valence Band Edge ~2.4 eV
XBL 847-7150

Figure 7

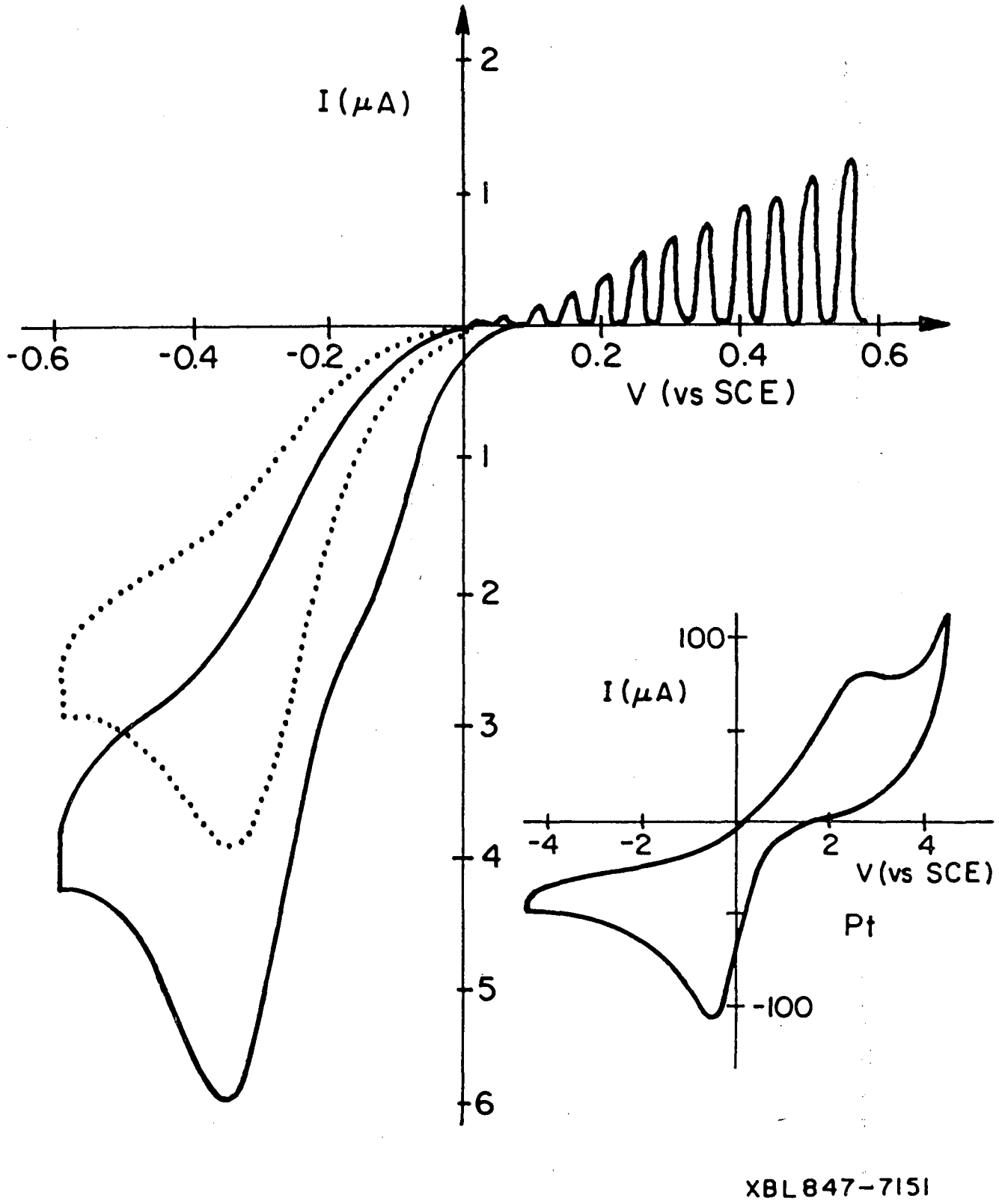
I (μA)
2
1
-0.6
-0.4
-0.2
0.2
0.4
0.6
V (vs SCE)
1
2
3
4
5
6
100
I (μA)
-4
-2
2
4
V (vs SCE)
Pt
-100
XBL847-7151

Figure 8

TECHNICAL INFORMATION DEPARTMENT
LAWRENCE BERKELEY LABORATORY
UNIVERSITY OF CALIFORNIA
BERKELEY, CALIFORNIA 94720